Local dissipation in driven Fermi gases

Tilman Enss and Keisuke Fujii
in collaboration with the Thywissen group

5 Oct 2023–30 May 2024

In an interacting Fermi gas, modulating the scattering length over time induces local dissipation. The rate of dissipation is governed by the bulk viscosity. A measurement of the heating rate determines the frequency-dependent bulk viscosity. A measurement of the phase shift of the time-dependent contact determines the viscous scattering time. In this way one can test the theoretical prediction of quantum critical dissipation in the unitary Fermi gas.

1 Local dissipation and bulk viscosity

When the scattering length is modulated in time, dissipative heating leads to a production of local energy density as [1]

$$\dot{\mathcal{E}}(\boldsymbol{r}) = \zeta(\boldsymbol{r}) \left[\nabla \cdot \boldsymbol{v}(\boldsymbol{r}, t) - d\, \frac{\dot{a}(t)}{a(t)} \right]^2 \tag{1}$$

for uniform $a(t)$ in dimension d. In the following we assume that the gas remains at rest during the drive with $\boldsymbol{v}(\boldsymbol{r}, t) = 0$ [1]. The heating rate is determined by the bulk viscosity ζ. The viscosity has units $\hbar n$, and because it scales as $1/a^2$ near unitarity is can be parametrized as

$$\zeta(n, T, a, \omega) = \frac{\hbar n}{(k_F a)^2}\, \tilde{\zeta}(n, T, \omega) = \frac{\hbar k_F}{3\pi^2 a^2}\, \tilde{\zeta}(\beta\mu, \beta\omega). \tag{2}$$

Here the dimensionless viscosity $\tilde{\zeta}$ is a function of the chemical potential and the driving frequency ω in temperature units. For trapped systems it is convenient to express also the density prefactor as a function of $\beta\mu$. This is achieved by using the equation of state

---

[1]It would be useful to estimate how large the velocity field would be if a trapped cloud expanded and contracted adiabatically with the drive to confirm this assumption.

(phase space density) $n\lambda^3 = f_n(\beta\mu)$, or equivalently $k_F\lambda = (3\pi^2 f_n)^{1/3}$ with thermal length λ and total density n for both spin components. Specifically, we can write

$$a^2\zeta(n,T,\omega) = \frac{\hbar}{\lambda}\frac{f_n^{1/3}(\beta\mu)}{(3\pi^2)^{2/3}}\tilde{\zeta}(\beta\mu,\beta\hbar\omega). \tag{3}$$

We have extracted the equation of state f_n from experimental data [2] and represent it numerically as a barycentric rational approximant.

Finally, the frequency dependence of the bulk viscosity is reported in [3]. We find that for small frequencies $\omega \lesssim \varepsilon_F$ the bulk viscosity follows approximately a Drude form,

$$\zeta(n,T,a,\omega) = \frac{\chi(n,T,a)\tau(n,T,a)}{1+\omega^2\tau^2(n,T,a)}, \qquad \tilde{\zeta}(\beta\mu,\beta\omega) = \frac{\tilde{\chi}\tau}{1+\omega^2\tau^2}. \tag{4}$$

The total spectral weight (bulk viscosity sum rule, scale susceptibility)

$$\chi = (2/\pi)\int_0^\infty d\omega\,\zeta(\omega) = (36\pi ma^2)^{-1}(\partial\mathcal{C}/\partial a^{-1})_{S,N} \tag{5}$$

is a thermodynamic property (denotes as S in [3]); in the second form $\tilde{\chi} = (2/\pi)\int_0^\infty d\omega\,\tilde{\zeta}(\beta\hbar\omega)$ has units of inverse time. The viscous relaxation time $\tau = \tilde{\zeta}(0)/\tilde{\chi}$ determines the width of the transport peak. Both the sum rule $\tilde{\chi}(\beta\mu)$ and the time $\tau(\beta\mu)$ are functions of the local fugacity, which we parametrize by rational approximants based on the data in Figs. 3(b,c) [3].

We find in particular that the relaxation rate

$$\tau^{-1} \approx (1.739 - 0.0892z + 0.00156z^2)\frac{k_BT}{\hbar} \tag{6}$$

is of order temperature and shows a very clear quantum critical scaling [4] up to high temperatures (the relaxation rate descreases appreciably only deep in the quantum degenerate regime $z \gg 1$). Typical values in the experimentally relevant temperature range are $\hbar\tau^{-1}/k_BT \approx 1.6$ for $z = 1.1$ ($T/T_F \approx 0.6$) and $\hbar\tau^{-1}/k_BT \approx 1.4$ for $z = 4.5$ ($T/T_F \approx 0.25$). Consequently, we find a quantum critical scaling regime where the relaxation rate depends linearly on temperature, but very little on density (fugacity). This theory prediction leads to dramatic simplifications in the description of the trapped gas, because the relaxation rate is nearly the same for a uniform and a harmonically trapped gas. While the thermodynamic properties depend on the density profile of the gas, the frequency dependence does not. If the frequency dependence is plotted vs ω/T, the normalized frequency dependence at different temperatures is expected to collaps onto a single curve.

At large frequencies $\omega \gtrsim \varepsilon_F$, instead, the frequency-dependent viscosity exhibits a contact tail

$$a^2\zeta(n,T,a,\omega) = \frac{\hbar^4\mathcal{C}(n,T,a)}{36\pi(m\hbar\omega)^{3/2}} \tag{7}$$

proportional to the contact density $\mathcal{C}(n,T,a)$. In the following we discuss two experimental protocols that probe local dissipation and bulk viscosity.

2 Dissipative heating in a driven gas

We consider a three-dimensional Fermi gas where the scattering length is modulated in time near unitarity,

$$a^{-1}(t) = a_{\mathrm{bf}}^{-1} + a_1^{-1} \sin(\omega t). \tag{8}$$

The modulation with frequency ω has amplitude a_1^{-1} around a background value a_{bg}^{-1} close to unitarity. The heating rate is then

$$\dot{\mathcal{E}} = 9(\partial_t a^{-1})^2 a^2 \zeta = \frac{9}{2} \frac{\omega^2}{a_1^2} a^2 \zeta, \tag{9}$$

where the factor $1/2$ gives the heating rate averaged over one cycle of the drive. At given μ, T and ω the heating rate can be expressed using (3) as

$$\dot{\mathcal{E}} = \frac{9}{2} \frac{\hbar \omega^2}{\lambda^3} A^2 \frac{f_n^{1/3}(\beta\mu)}{(3\pi^2)^{2/3}} \tilde{\zeta}(\beta\mu, \beta\omega), \tag{10}$$

where the dimensionless amplitude $A = \lambda/a_1$ denotes the amplitude of the scattering length drive in units of the thermal length.

In a homogeneous system the relative rate of energy change is obtained as $\dot{\mathcal{E}}/\mathcal{E}$, by normalizing with the internal energy density $\mathcal{E}$. In the unitary gas the energy density is given in terms of the pressure equation of state $f_p(\beta\mu)$ as

$$\mathcal{E} = \frac{3}{2}p = \frac{3}{2} f_p(\beta\mu) \lambda^{-3} k_B T. \tag{11}$$

From the pressure equation of state, the phase space density follows as the derivative $f_n(\beta\mu) = f_p'(\beta\mu)$. The relative heating rate is shown as the blue curve in Fig. 1.

In an inhomogeneous gas the total heating rate is obtained from an integration of local changes of energy density over volume:

$$\dot{E} = \int d^3r \, \dot{\mathcal{E}}(\boldsymbol{r}) = \frac{9}{2} \frac{\omega^2}{a_1^2} \int d^3r \, a^2 \zeta(\boldsymbol{r}). \tag{12}$$

In an anisotropic harmonic trapping potential $V(\boldsymbol{r}) = \frac{m}{2} \sum_i \omega_i^2 r_i^2$ the above expression for the homogeneous gas has to be integrated at fixed T and ω but position dependent local chemical potential $\mu(\boldsymbol{r}) = \mu - V(\boldsymbol{r})$. This is conveniently written as an integration over equipotential surfaces of energy $v = \beta V(\boldsymbol{r}) \in [0, \infty)$ with the weight function

$$w(v) = \frac{1}{\lambda^3} \int d^3r \, \delta\big(\beta V(\boldsymbol{r}) - v\big) = \frac{2}{\sqrt{\pi}} (T/\overline{\omega})^3 \sqrt{v} \, \Theta(v), \tag{13}$$

where $\overline{\omega} = (\omega_x \omega_y \omega_z)^{1/3}$ is the geometric mean trapping frequency. The resulting particle number (again the total for both components) is computed as

$$N = \int_0^\infty dv \, w(v) \, f_n(\beta\mu - v) \tag{14}$$

(for the ideal Fermi gas one would have $N = -2(T/\overline{\omega})^3 \text{Li}_3(-z)$ at fugacity $z = e^{\beta\mu}$). With this the global Fermi energy of an ideal gas is given by $E_F = \hbar\overline{\omega}(3N)^{1/3}$, and the global reduced temperature is $\Theta = k_B T/E_F$. The trapping potential energy is

$$E_{\text{trap}} = \int_0^\infty dv\, w(v)\, f_n(\beta\mu - v)\, v, \tag{15}$$

and in the equilibrium initial state the internal energy $E_{\text{internal}} = E_{\text{trap}}$ follows from the virial theorem at unitarity. Alternatively, the internal energy may be obtained by time of flight. Finally, the trap averaged heating rate (12) is computed as

$$\dot{E} = \frac{9}{2}\,\hbar\omega^2 A^2 \int_0^\infty dv\, w(v)\, \frac{f_n^{1/3}(\beta\mu - v)}{(3\pi^2)^{2/3}}\, \tilde{\zeta}(\beta\mu - v, \beta\hbar\omega). \tag{16}$$

The heating rate relative to the initial internal energy E is shown as the red curves in Fig. 1.

In the quantum critical region the trap integral (16) simplifies further: one can insert for the viscosity the Drude form (4), and the local relaxation time $\tau(\beta\mu - v) \approx \text{const} \times \hbar/k_B T$ is nearly independent of local chemical potential and can be pulled out of the integral to obtain

$$\dot{E} = \frac{9}{2} A^2 \frac{\hbar\omega \cdot \omega\tau}{1 + \omega^2\tau^2} \int_0^\infty dv\, w(v)\, \frac{f_n^{1/3}(\beta\mu - v)}{(3\pi^2)^{2/3}}\, \tilde{\chi}(\beta\mu - v). \tag{17}$$

The trap average of the scale susceptibility (sum rule) is independent of frequency, and the measurement of the upturn in the frequency dependence yields the quantum critical scattering rate τ^{-1}.

For the figures the following parameters are used: $\overline{\omega} = 2\pi \times 305\text{Hz}$ (the anisotropy does not matter at the level of the LDA), temperature $k_B T/h = 11\text{kHz}$, chemical potential $\mu/h = -3.8\text{kHz}$ in order to obtain a particle number of $N_\sigma = 40000$ per spin state with the unitary EOS and a global Fermi energy $E_F/h = 19\text{kHz}$, which results in a global reduced temperature of $\Theta = 0.58$ (red curves). For comparison a uniform gas is considered at the same reduced temperature $\theta = 0.58$, which now requires $\mu/h = 1.5\text{kHz}$ with the unitary EOS (blue curves). We observe that the trapped gas has a somewhat smaller heating rate than in the homogeneous case.

For small frequencies the heating rate increases quadratically from the ω^2 factor in Eq. (16), while at large frequencies $\omega \gtrsim T$ the $1/\omega^{3/2}$ tail of the viscosity is expected to lead to a much slower increase (this contact tail is not yet included in the numerics so that the curves seem to level out). All curves are plotted for $A = \lambda/a_1 = 1$; for the given value of temperature the thermal length is $\lambda \approx 7200 a_B$ in units of Bohr radius [check], and a larger amplitude in the drive of the scattering length should increase the heating rate.
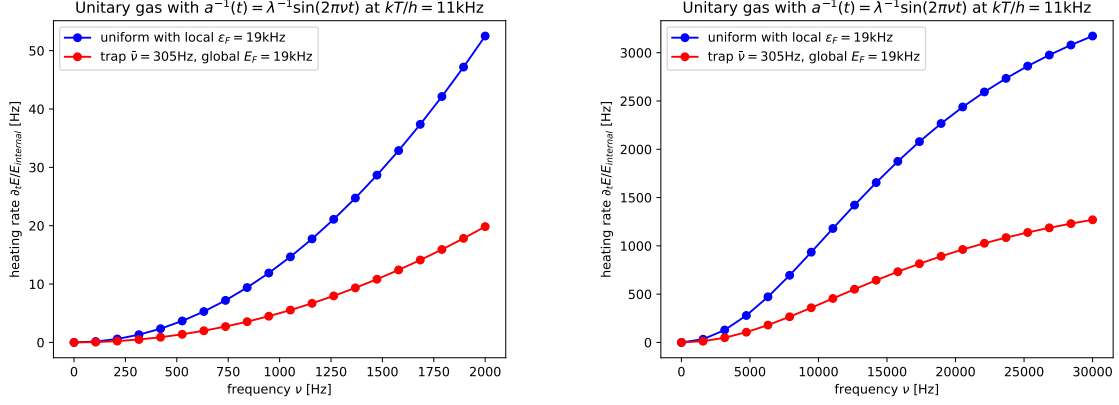
Figure 1: Heating rate of the modulated unitary Fermi gas at drive frequency $\omega = 2\pi\nu$ (left: smaller, right: larger frequencies) and amplitude $A = 1$.

3 Phase shift of contact for modulated scattering length

Following [1], a time dependent scattering length $a(t)$ leads to a time dependence of the contact density $\mathcal{C}(t)$, here in $d = 3$ dimensions:

$$\mathcal{C}(t) = \mathcal{C}_{\text{eq}}(a(t)) + 36\pi m \zeta \dot{a}(t) + \mathcal{O}(\delta^2 a, \delta \ddot{a}) \tag{18}$$

in terms of the equilibrium contact density $\mathcal{C}_{\text{eq}}(a)$ and the bulk viscosity $\zeta(n, T, a, \omega)$. We consider a scattering length that is modulated periodically as in Eq. (8). In response, also the contact density will oscillate with the same frequency. The dissipative term ζ leads to a phase lag with respect to the drive, which we will estimate in the following.

For small drive amplitude the equilibrium contact density will change to linear order depending on the sum rule χ (5),

$$\mathcal{C}_{\text{eq}}(a^{-1}(t)) = \mathcal{C}_{\text{eq}}(a_{\text{bg}}^{-1}) + a_1^{-1} \sin(\omega t) \frac{\partial \mathcal{C}(a^{-1})}{\partial a^{-1}}\bigg|_{a_{\text{bg}}^{-1}} \tag{19}$$

$$= \mathcal{C}_{\text{eq}}(a_{\text{bg}}^{-1}) + a_1^{-1} \sin(\omega t)\, 36\pi m a^2 \chi(a_{\text{bg}}^{-1}). \tag{20}$$

We thus find for the contact density

$$\mathcal{C}(t) = \mathcal{C}_{\text{eq}}(a_{\text{bg}}^{-1}) + 36\pi a_1^{-1} m a^2 \chi(a_{\text{bg}}^{-1}) \sin(\omega t) - 36\pi a_1^{-1} m \omega a^2 \zeta(a_{\text{bg}}^{-1}) \cos(\omega t) \tag{21}$$

$$= \mathcal{C}_{\text{eq}}(a_{\text{bg}}^{-1}) + \frac{6}{\pi} a_1^{-1} k_F^3 \left[\frac{(k_F a)^2 \chi}{n \varepsilon_F} \sin(\omega t) - \frac{\hbar \omega}{\varepsilon_F} \frac{(k_F a)^2 \zeta}{\hbar n} \cos(\omega t) \right]. \tag{22}$$

We define the dimensionless frequency-dependent viscosity $\tilde{\zeta} = (k_F a)^2 \zeta(\omega)/\hbar n$ plotted in Fig. 3a of [3] and the dimensionless scale susceptibility $x = (k_F a)^2 \chi / n \varepsilon_F = \hbar \tilde{\chi}/\varepsilon_F$ plotted in Fig. 3c (solid), as well as the dimensionless contact density $c = \mathcal{C}/k_F^4$ plotted

5

in Fig. 3c (dotted), and find (with $A = \lambda/a_1$ as before)

$$c(t) = c_{\mathrm{eq}}(a_{\mathrm{bg}}^{-1}) + \frac{6}{\pi} \frac{A}{k_F \lambda} \left[x \sin(\omega t) - \frac{\hbar\omega}{\varepsilon_F} \tilde{\zeta} \cos(\omega t) \right] \tag{23}$$

$$= c_{\mathrm{eq}}(a_{\mathrm{bg}}^{-1}) + \frac{6}{\pi} \frac{A}{(3\pi^2 f_n)^{1/3}} \sqrt{x^2 + (\hbar\omega/\varepsilon_F)^2 \tilde{\zeta}^2} \, \sin(\omega t - \varphi). \tag{24}$$

The oscillations have amplitude $\frac{6Ax}{\pi \cos(\varphi)}$ directly proportional to the drive A (in contrast to the dissipative heating, which scales as A^2) and a dissipative phase shift

$$\varphi = \arctan\left(\frac{\hbar\omega}{\varepsilon_F} \frac{\tilde{\zeta}}{x}\right) = \arctan\left(\frac{\omega\zeta(\omega)}{\chi}\right) = \arctan\left(\frac{\omega\zeta(\omega)}{\frac{2}{\pi} \int_0^\infty d\omega \, \zeta(\omega)}\right). \tag{25}$$

For low frequencies in the Drude regime (4) this simplifies further to

$$\varphi = \arctan\left(\frac{\omega\tau}{1 + (\omega\tau)^2}\right). \tag{26}$$

The frequency-dependent phase shift is fully determined by the scattering time τ as the only parameter, which can be read off either from the slope at small frequency or from the frequency $\omega = 1/\tau$ where the maximum $\varphi_{\mathrm{max}} = \arctan\frac{1}{2} \simeq 0.464$ is reached. The phase shift for a typical temperature $T/T_F = 0.58$ is shown in Fig. 2. Indeed, the phase shift initially increases linearly with frequency and peaks at a frequency of $\omega\tau = 1$, or $\omega \approx 1.6T \approx 18\mathrm{kHz}$ as predicted for quantum critical dissipation.

For the trapped gas one has to perform a trap average both of the instantaneous and the equilibrium contact:

$$C(t) = \int d^3r \, \mathcal{C}(\boldsymbol{r}, t), \qquad\qquad C_{\mathrm{eq}} = \int d^3r \, \mathcal{C}_{\mathrm{eq}}(\boldsymbol{r}). \tag{27}$$

Applying the trap average to the density dependent terms in Eq. (22) we obtain

$$\bar{x} \sin(\omega t) - \bar{z} \cos(\omega t) \propto \sin(\omega t - \varphi) \quad \text{with} \quad \varphi = \arctan(\bar{z}/\bar{x}) \tag{28}$$

in terms of the trap averaged bulk viscosity $\bar{z}$ and sum rule $\bar{x}$,

$$\bar{z} = \frac{1}{4\pi} \int d^3r \, \frac{\hbar\omega k_F^3}{\varepsilon_F} \tilde{\zeta}(\beta\mu - V(\boldsymbol{r}), \beta\hbar\omega) \tag{29}$$

$$= \beta\omega \int_0^\infty dv \, w(v) \, (3\pi^2 f_n(\beta\mu - v))^{1/3} \, \tilde{\zeta}(\beta\mu - v, \beta\hbar\omega), \tag{30}$$

$$\bar{x} = \frac{1}{4\pi} \int d^3r \, \frac{\hbar k_F^3}{\varepsilon_F} \tilde{\chi}(\beta\mu - V(\boldsymbol{r})) \tag{31}$$

$$= \int_0^\infty dv \, w(v) \, (3\pi^2 f_n(\beta\mu - v))^{1/3} \, \frac{\hbar}{k_B T} \tilde{\chi}(\beta\mu - v). \tag{32}$$

Due to the density weighted integrals the trap averaged phase shift is not the same as in the uniform system. However, it is remarkably close in the quantum critical regime.

Indeed, we found above that the bulk viscous scattering rate $\tau^{-1} \simeq 1.6\,\hbar/k_B T$ is largely independent of density or $\beta\mu$. If we insert the Drude form (4) for the bulk viscosity then only the sum rule depends on density and we can pull the $\omega\tau$ factors outside the trap average to obtain

$$\bar{z} = \frac{\omega\tau}{1+(\omega\tau)^2} \int_0^\infty dv\, w(v)\, (3\pi^2 f_n(\beta\mu - v))^{1/3} \frac{\hbar}{k_B T}\, \tilde{\chi}(\beta\mu - v) = \frac{\omega\tau}{1+(\omega\tau)^2}\, \bar{x}, \quad (33)$$

which has exactly the same density dependence as $\bar{x}$. Therefore, the density dependence cancels in the phase shift and we find

$$\varphi = \arctan\left(\frac{\omega\tau}{1+(\omega\tau)^2}\right) \tag{34}$$

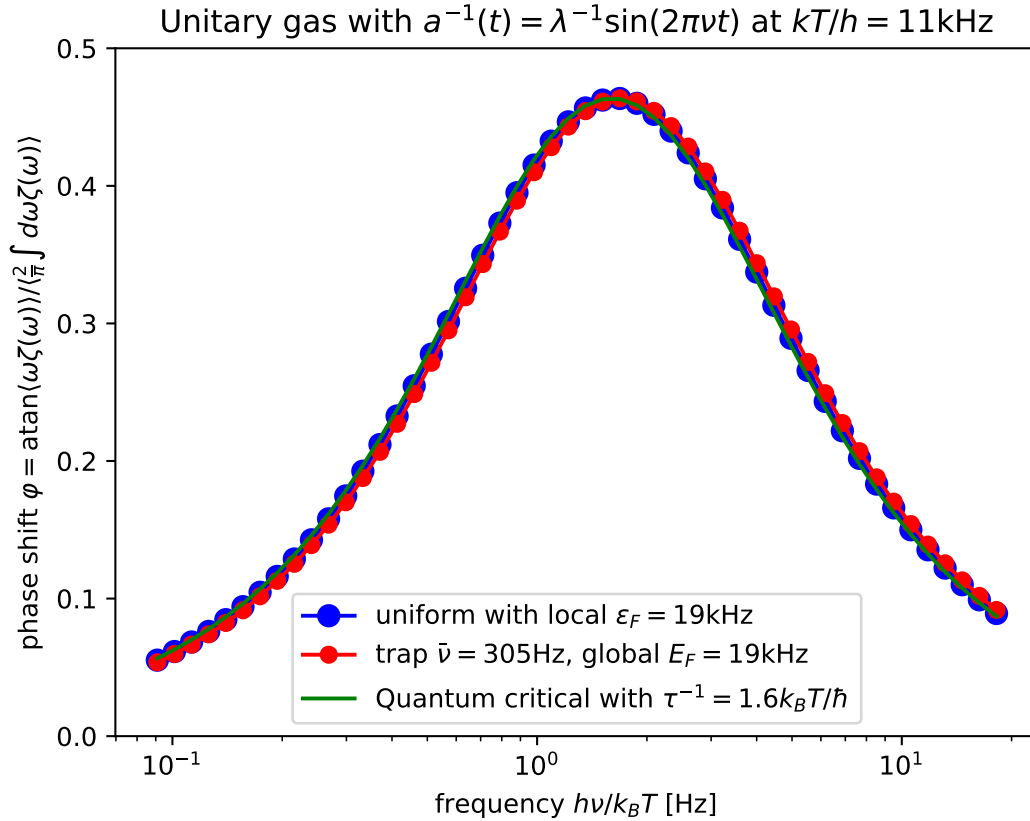in the quantum critical regime *also in the harmonically trapped gas.*

Figure 2: Phase shift φ at unitarity as a function of drive frequency ν at $T/T_F = 0.58$. The uniform and trapped results agree almost perfectly, which is a consequence of the quantum critical scattering rate $\tau^{-1} \approx 1.6\,T \sim 18\text{kHz}$ independent of density (see text).

4 Theory predictions for the trapped gas

To summarize, the theory predictions for the heating rate and phase shift are as follows. The heating rate at high frequency is proportional to the contact, and the ratio of heating rate to contact scales as $\omega^{1/2}$ and drive amplitude squared (with units $(\hbar k_F)^3/m^2$):

$$\frac{\dot{E}}{C} = \frac{\hbar^2(m\hbar\omega)^{1/2}}{8\pi m^2 a_1^2}. \tag{35}$$

In the Drude regime, instead, one has $\zeta = \chi\tau/(1+\omega^2\tau^2)$. One obtains the trap average of the scale susceptibility $\chi = \frac{(\partial\mathcal{C}/\partial a^{-1})_{S,N}}{36\pi ma^2}$ (5) from the measured values of the contact for different scattering length (at constant entropy),

$$\int d^3r\, a^2\chi = \frac{1}{36\pi m}\left(\frac{\partial C}{\partial a^{-1}}\right)_{S,N}. \tag{36}$$

Then

$$\frac{\dot{E}}{\int d^3r\, a^2\chi} = \frac{9}{2}\frac{\omega^2}{a_1^2}\frac{\int d^3r\, a^2\chi\,\frac{\tau}{1+\omega^2\tau^2}}{\int d^3r\, a^2\chi} \tag{37}$$

$$= \frac{9}{2}a_1^{-2}\frac{\omega^2\tau}{1+\omega^2\tau^2}. \tag{38}$$

In the last line we used the prediction of quantum critical dissipation to pull τ out of the integral.

Similarly for the phase shift, in the quantum critical regime one predicts

$$\tan\varphi = \frac{\omega\tau}{1+\omega^2\tau^2} \tag{39}$$

independent of the density profile in the trap. This form reveals the quantum critical scattering rate $\tau^{-1} \propto T$. In order to test the quantum critical prediction one should plot $\tan\varphi$ vs ω/T (as in Fig. 2) for different temperatures: the prediction is that all these curves collapse onto a single one. The position of the maximum, or equivalently the slope at small frequency, reveals the unique quantum critical scattering rate. It will be useful to record the full time series data, also immediately after the modulation starts, for future tests of hydrodynamics [5].

References

[1] K. Fujii and Y. Nishida, *Hydrodynamics with spacetime-dependent scattering length*, Phys. Rev. A **98**, 063634 (2018).

[2] M. J. H. Ku, A. T. Sommer, L. W. Cheuk, and M. W. Zwierlein, *Revealing the Superfluid Lambda Transition in the Universal Thermodynamics of a Unitary Fermi Gas*, Science **335**, 563 (2012).

[3] T. Enss, *Bulk Viscosity and Contact Correlations in Attractive Fermi Gases*, Phys. Rev. Lett. **123**, 205301 (2019).

[4] T. Enss and J. H. Thywissen, *Universal Spin Transport and Quantum Bounds for Unitary Fermions*, Annu. Rev. Condens. Matter Phys. **10**, 85 (2019).

[5] K. Fujii and T. Enss, *Hydrodynamic attractor in ultracold atoms*, arXiv:2404.12921 (2024).